Mon. Not. R. Astron. Soc. **363,** L76–L80 (2005) doi:10.1111/j.1745-3933.2005.00086.x

GRB 050223: a faint gamma-ray burst discovered by *Swift*

K. L. Page,[1⋆] E. Rol,[1] A. J. Levan,[1] B. Zhang,[2] J. P. Osborne,[1] P. T. O'Brien,[1] A. P. Beardmore,[1] D. N. Burrows,[3] S. Campana,[4] G. Chincharini,[4,5] J. R. Cummings,[6] G. Cusumano,[7] N. Gehrels,[6] P. Giommi,[8] M. R. Goad,[1] O. Godet,[1] V. Mangano,[6] G. Tagliaferri[4] and A. A. Wells[1]

[1]*X-Ray and Observational Astronomy Group, Department of Physics & Astronomy, University of Leicester, Leicester LE1 7RH*
[2]*University of Nevada, Box 454002, Las Vegas, NV 89154-4002, USA*
[3]*Department of Astronomy & Astrophysics, 525 Davey Lab, Pennsylvania State University, University Park, PA 16802, USA*
[4]*INAF – Osservatorio Astronomico di Brera, Via Bianchi 46, 23807 Merate, Italy*
[5]*Università degli studi di Milano–Bicocca, Dipartimento di Fisica, Piazza delle Scienze 3, I-20126 Milano, Italy*
[6]*NASA Goddard Space Flight Center, Greenbelt, MD 20771, USA*
[7]*INAF – Istituto di Astrofisica Spaziale e Fisica Cosmica Sezione di Palermo, Via Ugo La Malfa 153, 90146 Palermo, Italy*
[8]*ASI Science Data Centre, via Galileo Galilei, 00044 Frascati, Italy*

Accepted 2005 July 26. Received 2005 July 22; in original form 2005 June 8

ABSTRACT

GRB 050223 was discovered by the *Swift Gamma-Ray Burst Explorer* on 2005 February 23 and was the first gamma-ray burst (GRB) to be observed by both *Swift* and *XMM–Newton*. At the time of writing (2005 May), it has one of the faintest GRB afterglows ever observed. The spacecraft could not slew immediately to the burst, so the first X-ray and optical observations occurred approximately 45 min after the trigger. Although no optical emission was found by any instrument, both *Swift* and *XMM–Newton* detected the fading X-ray afterglow. Combined data from both of these observatories show the afterglow to be fading monotonically as $0.99^{+0.15}_{-0.12}$ over a time-frame between 45 min and 27 h post-burst. Spectral analysis, allowed largely by the higher throughput of *XMM–Newton*, implies a power law with a slope of $\Gamma = 1.75^{+0.19}_{-0.18}$ and shows no evidence for absorption above the Galactic column of 7×10^{20} cm^{-2}.

From the X-ray decay and spectral slopes, a low electron power-law index of $p = 1.3$–1.9 is derived; the slopes also imply that a jet-break has not occurred up to 27 h after the burst. The faintness of GRB 050223 may be due to a large jet opening or viewing angle or a high redshift.

Key words: gamma-rays: bursts.

1 INTRODUCTION

The *Swift Gamma-Ray Burst Explorer* (Gehrels et al. 2004) was launched on 2004 November 20. It is a multi-wavelength observatory, covering the gamma-ray, X-ray and ultraviolet/optical bands. The observatory is designed to slew rapidly and autonomously to point narrow-field instruments (the X-ray and Ultra-Violet/Optical Telescopes – XRT and UVOT, respectively) towards any gamma-ray bursts (GRBs) detected by the Burst Alert Telescope (BAT). This allows prompt observations of the afterglow on a time-scale of minutes, much more quickly than was previously feasible on a regular basis. The on-board instruments are described in detail by Barthelmy et al. (2004, 2005, BAT), Burrows et al. (2004, 2005, XRT) and Roming et al. (2004, 2005, UVOT).

Swift is significantly more sensitive to the detection of GRBs than previous instruments capable of providing rapid, accurate (to within a few arcmin) localizations (e.g. *HETE-2* and *BeppoSAX*). Thanks to its rapid repointing capability, *Swift* is also able to observe afterglows at early times. Since GRB afterglows fade rapidly, this ensures that they are observed at their brightest, allowing *Swift* to detect fainter afterglows and thus look further down the GRB afterglow luminosity function than has previously been possible. Investigating the faint end of this function is of particular importance in understanding the structure of the bursts themselves. Faint bursts may be manifestations of many different effects, such as a large luminosity distance [*Swift* should be able to detect bursts out to $z \sim 15$–20 (Lamb & Reichart 2000)] or differences in the fireball emission (shock generation, jet structure). Alternatively, they could be due to a separate population of low-luminosity, relatively nearby ($z < 0.2$) bursts (e.g. Sazonov, Lutovinov & Sunyaev 2004). The combined study of the prompt and afterglow emission

⋆E-mail: kpa@star.le.ac.uk

of these bursts will make it possible to distinguish between these possibilities.

Here results of *Swift* and *XMM–Newton* observations of GRB 050223, which has one of the faintest X-ray afterglows to date, are presented and constraints are placed on some of the burst and afterglow parameters.

2 OBSERVATIONS

GRB 050223 (*Swift* Trigger 106709) was detected by the *Swift* BAT at 03:09:06 UT on 2005 February 23 (Mitani et al. 2005), at a location of RA (J2000) = $18^{\rm h}05^{\rm m}34^{\rm s}$, Dec. (J2000) = $-62^\circ28'52''$, with an uncertainty of 4 arcmin; the burst was also detected by *INTEGRAL* (Mereghetti et al. 2005). Because of the Earth-limb constraint, the *Swift* spacecraft could not slew to the BAT position until 03:44 UT, at which point the observatory was in the South Atlantic Anomaly (SAA). The XRT began collecting data upon exiting the SAA, at 03:56:37 UT. An uncatalogued X-ray source was identified at RA (J2000) = $18^{\rm h}05^{\rm m}32\overset{\rm s}{.}6$, Dec. (J2000) = $-62^\circ28'19\overset{''}{.}7$, with an uncertainty of 8 arcsec (Giommi et al. 2005); this is 33 arcsec from the BAT position. The UVOT began observations slightly before the XRT, at 03:55:28 UT.

Since this GRB was detected during the calibration phase of *Swift*, the XRT was in manual state, where data-mode switching is not automatically enabled; there were, therefore, no automatic alerts sent out via the Tracking and Data-Relay Satellite System (TDRSS). Also, during the initial observation all data were obtained in photon counting (PC) mode, rather than the standard cycle starting with an image mode frame.

Swift software version 1.2 was used to process the XRT and BAT data. The BAT files were processed using the latest version (2.17) of the analysis script, which produces mask-weighted spectra and light curves. For the XRT, events below a threshold of 80 Digital Number (DN) (approximately 0.2 keV) were filtered out and the bad pixels removed. This method ensures that the event file is as clean as possible, removing the effects of the sunlit Earth, and is the default pipeline method for later releases of the software.

Source and background spectra were then extracted using a circular region of radius 15 pixel (1 pixel = 2.36 arcsec). Only grade 0 events were used for the XRT PC mode spectra, since the response matrix (RMF) for these single-pixel events (swxpc0_20010101v006.rmf) was the best calibrated at the time of analysis; using all calibrated grades (0–12) did not significantly improve the statistics. Grades 0–12 were used for the light curves, however. The FTOOL XRTMKARF was used to generate suitable ancillary response function (ARF) files for the spectral fitting.

XMM–Newton also observed the field of GRB 050223 (Gonzalez-Riestra et al. 2005; Rodriguez 2005; De Luca & Campana 2005). SAS v6.1 was used for these data, choosing patterns (equivalent to *Swift* grades) 0–12 for MOS and 0–4 for PN. Background light curves showed frequent flaring for the later *XMM–Newton* observation, particularly in the PN data, so a small source extraction radius (35 arcsec) was used in addition to screening out the worst of the background contribution. The SAS tasks RMFGEN and ARFGEN were then run to produce the RMF and ARF files respectively.

All spectra were grouped to a minimum of 20 counts per bin, in order to facilitate χ^2 fitting in XSPEC v11.3.1. Throughout this Letter, errors are given at the 90 per cent level (e.g. $\Delta\chi^2 = 2.7$ for one degree of freedom).

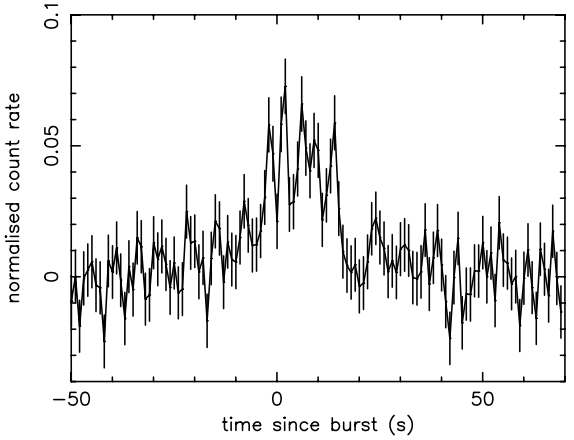

Figure 1. The BAT light curve, over 15–350 keV, with 1-s binning.

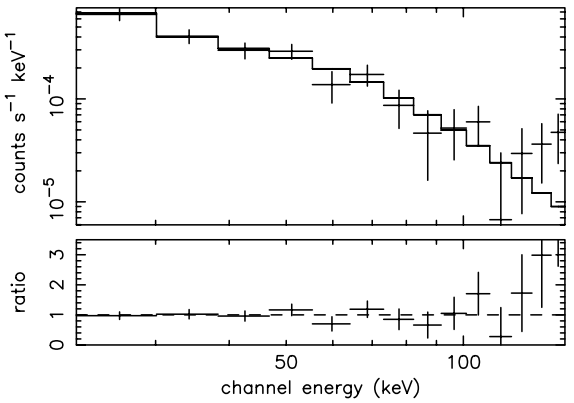

Figure 2. The BAT spectrum can be fitted with a simple power-law model, with $\Gamma_\gamma \approx 1.85$.

2.1 Gamma-ray data

The BAT light curve of GRB 050223 shows a slow rise and fall, with several short peaks superimposed (Mitani et al. 2005; Fig. 1). T_{90} for this burst is 23 s, while the peak flux, over a 1-s interval, was 0.8 photon cm^{-2} s^{-1} (15–350 keV; Mitani et al. 2005).

The *INTEGRAL* IBIS/ISGRI instrument also detected GRB 050223, measuring a peak flux (1-s integration) of 0.6 photon cm^{-2} s^{-1} over 20–200 keV (Mereghetti et al. 2005).

A single power law gave a good fit (χ^2/d.o.f. = 48/57; Fig. 2) for $\Gamma_\gamma = 1.85 \pm 0.19$,[1] which was not improved upon by using the Band model (Band et al. 1993). The energy fluence over 15–350 keV was 9.69×10^{-7} erg cm^{-2}, placing it in the lowest third of the *Swift*-measured fluence distribution.

2.2 X-ray data

Table 1 lists the times and durations of the X-ray data obtained from *Swift* and *XMM–Newton*. All the useful *Swift* data were obtained in PC mode, for both the initial (three orbits of data) and second (seven orbits when settled on the source) observations. The *XMM–Newton*

[1] When considering spectral slopes in X-ray astronomy, the convention is to give the value as Γ, the photon index, where $f(E) \propto E^{-\Gamma}$; $f(E)$ is in units of photon cm^{-2} s^{-1}.

Table 1. Exposure times for the *Swift*–XRT (PC mode) and *XMM–Newton* –MOS data. The burst trigger time from the BAT was 2005-02-23T03:09:06 UT. The first *Swift* observation corresponds to sequence number 00106709000; the second to 00106709001. The first and second *XMM–Newton* observations correspond to before and after a ground station outage between 2005-02-23T16:54 and 2005-02-23T18:56 UT.

Instrument	Observation	Orbit	Start time (s after BAT trigger)	End time (s after BAT trigger)
Swift–XRT	1	1	2847	3973
Swift–XRT	1	2	9150	9710
Swift–XRT	1	3	14665	15475
Swift–XRT	2	1–7	38265	73530
XMM–MOS1/MOS2	3	–	35 746/35 745	49 526/49 533
XMM–MOS1/MOS2	4	–	57 450/57 527	96 452/96 456

MOS1 and MOS2 data were checked for consistency and then co-added for subsequent analysis. The *XMM–Newton* PN data are more badly affected by the high background, so are not presented here, but the results are in agreement with the MOS.

2.2.1 *Light-curve analysis*

Because of the location of GRB 050223, most of the *Swift*–XRT pointings were close to the Earth limb (small 'bright Earth' angles). This led to a high optical background in the field of view which, together with the afterglow being faint, complicated the X-ray data analysis.

Light curves were extracted for each individual orbit of data. Because of the faintness of the afterglow, there were very few counts in each of the orbit bins (Table 2) so, in order to improve the statistics, a large background region was used (a circle of radius 60 pixel) and the number of background counts scaled down to the size of the source region (radius 15 pixel). The count rates were corrected for the fractional exposure where required. As Fig. 3 shows, only the first two orbits of data show count rates significantly above the background level of around 2.7×10^{-3} count s^{-1} (within the 15 pixel radius circle). Considering the second *Swift* observation as a whole, the source is detected at the 3σ level (using the DETECT command in XIMAGE).

In order to compare the data from *XMM–Newton* (observation ID 0164570601) with the *Swift* results, the light curve has to be plotted in terms of flux using the spectral fit given in Section 2.2.2, rather than count rate, because of the differences between the two instruments. The background for the *XMM–Newton* MOS detectors was checked and found to be about one-third the count rate of the source before the ground station outage, and about half afterwards, so the burst is clearly detected. A combined light curve of the *Swift* and *XMM–Newton* observations is plotted in Fig. 4, showing a decay

Table 2. The number of source counts (to one decimal place) for each *Swift*–XRT observation, integrated over each orbital time-bin. The last column gives the fraction of the time-bin during which data were actually collected.

Obs. number	Orbit number	Source counts	Time-bin (s)	Exposure fraction
1	1	24.3	1125	0.89
1	2	3.7	560	0.96
1	3	2.4	810	0.84
2	1	1.7	400	1.0
2	2	2.6	495	1.0
2	3	0.7	385	1.0
2	4	2.8	380	1.0
2	5	0.7	340	1.0
2	6	1.7	525	1.0
2	7	1.6	590	1.0

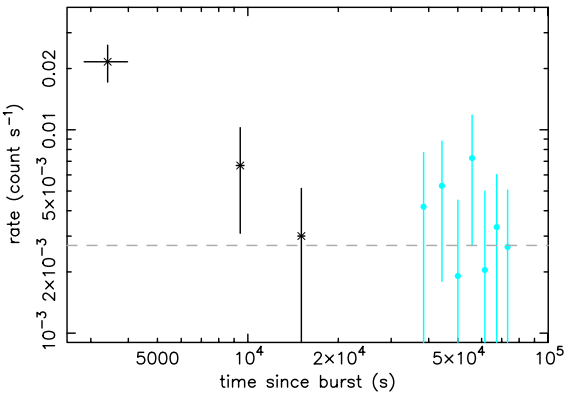

Figure 3. *Swift*–XRT light curves for each orbit of GRB 050223 data; the first three points (marked with asterisks) show data from sequence number 00106709000; the following seven points (circles) are from 00106709001. The dashed horizontal line shows the background level; with the exception of the data from the first two orbits, the burst is not significantly detected above the background in individual orbit segments.

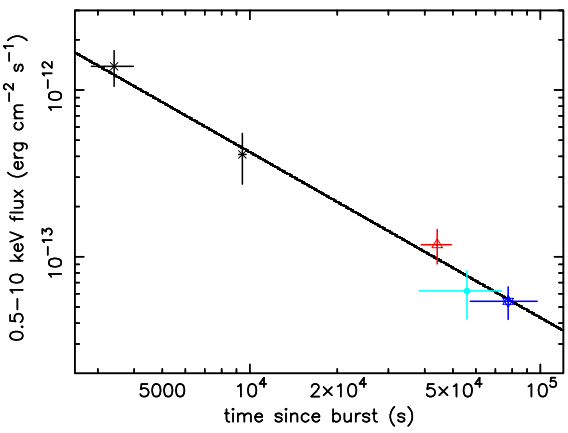

Figure 4. Plotting the light curve in terms of flux, the *XMM–Newton* measurements can be compared with those from *Swift*. The asterisks show the first two orbits of *Swift* data (within observation 1) and the circle the whole of the second *Swift* observation, while the *XMM–Newton* points are marked by a triangle and a star (observations 3 and 4 respectively). The model shown is a decay slope of 0.99.

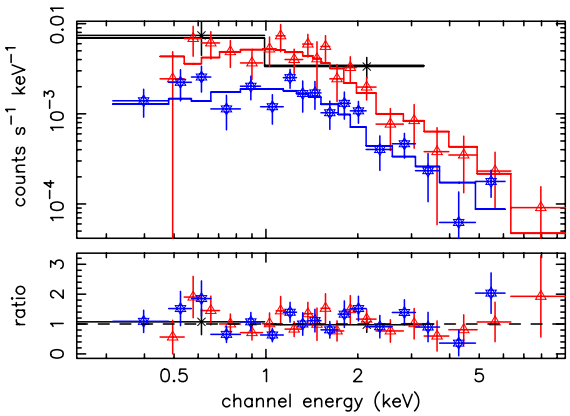

Figure 5. A power-law fit ($\Gamma \approx 1.75$) to the joint *Swift*–XRT (asterisks) and *XMM–Newton* (triangles and stars for observations 3 and 4 respectively) data. The *Swift* spectrum was formed from the first three orbits of data. The spectrum from the second *Swift* observation consists of a single bin of data, so has not been included.

slope[2] of $\alpha = 0.99^{+0.15}_{-0.12}$. The second *Swift* observation occured simultaneously with the *XMM–Newton* observations, with the values from the different satellites being in good agreement.

2.2.2 *Spectral analysis*

Because of the faintness of the X-ray afterglow and the high optical background, the *Swift*–XRT spectrum is of low statistical quality. However, simultaneously fitting the spectrum, derived from the three orbits in the first observation, and the co-added *XMM–Newton*–MOS spectra produces a good fit (χ^2/d.o.f. = 28/34; Fig. 5) for a single power law of $\Gamma = 1.75^{+0.19}_{-0.18}$ absorbed by the Galactic column of 7×10^{20} cm^{-2} (Dickey & Lockman 1990), with a different constant of normalization between the individual spectra. No change in spectral shape is found between the *XMM–Newton* spectra.

Note that the spectrum is shown in detected count s^{-1} keV^{-1} for each of the instruments. Thus, while the *XMM–Newton* spectrum may have a higher count rate, due to the higher throughput, this does not correspond to an increased flux.

The unabsorbed fluxes (0.5–10 keV) for observations 1, 3 and 4 (as named in Table 1) were found to be $(8.18^{+3.32}_{-2.74}) \times 10^{-13}$, $(1.18^{+0.19}_{-0.36}) \times 10^{-13}$ and $(5.42^{+0.98}_{-1.44}) \times 10^{-14}$ erg cm^{-2} s^{-1} respectively.

2.3 Ultraviolet and optical data

Neither the *Swift*–UVOT (Gronwall et al. 2005) nor the *XMM–Newton* Optical Monitor (OM) (Blustin et al. 2005) detected a source at the position of the X-ray afterglow. As mentioned above, the UVOT observation started about 46 min after the BAT trigger, because of the delayed slew; the *XMM–Newton*–OM data were collected 11 h after the trigger.

No new sources were identified by ROTSE-III (to a limiting unfiltered magnitude of 18 from approximately a minute after the burst: Smith 2005), the Mount John University Observatory (to $R = 20.5$, 10 h after the burst: Gorosabel et al. 2005) or the PROMPT robotic telescope array (limiting magnitude of ≈21 for *R*c, *V* and *I*c filters, with the mean time for these observations being 4–5 h after the trigger: Nysewander et al. 2005).

3 DISCUSSION

GRB 050223 has, at the time of writing (2005 May), one of the faintest GRB X-ray afterglows observed by *Swift*; comparison with fig. 1 of Piro (2004) shows the 11-h flux of GRB 050223 to be below all those detected by *BeppoSAX*.

3.1 Afterglow models

Three GRB afterglow models are initially considered, as summarized by Zhang & Mészáros (2004). The 'ISM' model has a fireball expanding into the (homogeneous) interstellar medium (Sari, Piran & Narayan 1998), while, in the 'wind' model, the fireball expands into a wind environment, with the density $\rho \propto r^{-2}$ (Chevalier & Li 1999). In these models the beaming angle ($1/\Gamma_0$, where Γ_0 is the Lorentz factor; this is simply the cone into which the emission is beamed as a result of relativistic effects) is less than any jet opening angle. As the jet slows down, $1/\Gamma_0$ will become larger; when it becomes equal to the opening angle, a transition, known as the jet-break, is seen. At this point, the emission observed decreases because of both the edge effect (less emission per unit solid angle is seen) and the sideways spreading of the causally connected region. These effects may not happen simultaneously, but are thought to be close in time (Panaitescu & Mészáros 1999; Sari, Piran & Halpern 1999). The third model is for post-jet-break evolution, when the finite angular extent of the jet dominates (Sari et al. 1999), which is valid for both the ISM and wind cases.

The reasonable assumptions that the X-ray afterglow lies above the synchrotron injection frequency (ν_m) and that during the XRT observations, hours after the GRB, slow cooling is effective (i.e. $\nu_X > \nu_c$, the X-ray frequency is greater than the cooling frequency) are made. Then the afterglow temporal decay and spectral indices ($\alpha = 0.99^{+0.15}_{-0.12}$ and $\Gamma = 1.75^{+0.19}_{-0.18}$) indicate an electron power-law index $p = 1.3$–1.9 for a spherical blast wave since $\alpha = (3p + 10)/16$ for the ISM case, $(p + 6)/8$ for wind cooling and $(p + 6)/4$ for the jet-dominated case, while Γ is given by $1 + (p/2)$ for each (Dai & Cheng 2001).

The data are consistent with either an ISM or wind regime. For jet-dominated evolution the high-frequency emission falls off as $t^{-(p+6)/4}$, much more steeply than the decay observed in GRB 050223. As might be expected for these relatively early observations, our spectral and temporal slopes are inconsistent with post-jet-break evolution.

A value of p less than 2 is not generally thought to be physical (e.g. Panaitescu & Kumar 2001), although possible ways to generate such a flat spectrum have been suggested (e.g. Bykov & Mészáros 1996). A similarly low value for p was among the possibilities for GRB 050128 (Campana et al. 2005) if the observed change in slope of the decay curve was caused by a jet-break in that burst.

A jet-break in the light curve for a large opening angle would naturally occur at a late time (Piran 1999). A late jet-break is in agreement with the analysis above, which indicates that the outflow prior to the jet-break is being observed, with no indication of such a break up to at least 10^5 s. Jet-breaks are frequently observed at longer than a day after the burst (see e.g. Frail et al. 2001), so this is not unusual. A large opening angle could also explain the relative faintness of the X-ray afterglow and the BAT fluence being at the lower end of the *Swift* fluence distribution.

[2] $f(t, \nu) \propto t^{-\alpha}\, \nu^{-\beta}$ where $\beta = \Gamma - 1$.

The GRB jet opening angle can be estimated to be $\theta_j \approx 0.35$–0.4 rad using the observed correlations of gamma-ray fluence and X-ray afterglow decay index with a jet opening angle measured by jet-break times for 10 GRBs by Liang (2004). Our jet angle estimate is relatively large compared with the sample of Frail et al. (2001). It should, however, be noted that the Liang relationships were derived from a sample of only 10 bursts and doubts about their general applicability remain. Also, Bloom, Frail & Kulkarni (2003) list bursts (e.g. GRB 000418 and 021004) that are bright, yet have larger than typical opening angles.

If GRB 050223 produced a structured jet [that is, $\Gamma(\theta) \propto \theta^{-q}$], then the faintness seen here could be due to a large viewing angle from the jet axis. In this case the viewing angle corresponds to a low energy density in the jet. The absence of a jet-break before one day in our data is consistent with an off-axis viewing angle (Zhang & Mészáros 2002; Rossi, Lazzati & Rees 2002).

Alternatively, the observed low afterglow flux and prompt fluence could be explained by GRB 050223 being at high redshift. In this case, any jet-break is delayed by a factor proportional to $1 + z$. Indeed, *Swift* bursts to date are on average fainter than those detected by *BeppoSax* and *HETE-2* (Piro 2004; Berger et al. 2005) and the median redshift of the six *Swift* bursts for which it has been measured so far is large, at $z = 2.4$, compared with a median $z = 1.0$ for non-*Swift* bursts.[3]

4 SUMMARY

Observations by *Swift* and *XMM–Newton* have shown GRB 050223 to have faint prompt gamma-ray and X-ray afterglow emission. The X-ray data agree with the standard stellar wind and constant circumstellar density afterglow models if the electron power-law index $p = 1.3$–1.9. A jet-break does not appear to have occurred up to one day after the burst. The faintness of GRB 050223 may be due to a large jet opening or viewing angle, or a high redshift.

ACKNOWLEDGMENTS

We thank Don Lamb for useful comments on the paper, and Jochen Greiner for his GRB afterglows website. This work is supported at the University of Leicester by the Particle Physics and Astronomy Research Council (PPARC), at Penn State by NASA contract NAS5-00136 and in Italy by funding from ASI (contract number I/R/039/04). JRC is supported by a National Research Council Associateship award at NASA's Goddard Space Flight Center.

[3] Values taken from Jochen Greiner's website at http://www.mpe.mpg.de/~jcg/grbgen.html

REFERENCES

Band D. et al., 1993, ApJ, 413, 281
Barthelmy S. D. et al., 2004, Proc. SPIE, 5165, 175
Barthelmy S. D. et al., 2005, Space Sci. Rev., in press (astro-ph/0507410)
Berger E. et al., 2005, ApJ, in press (astro-ph/0505107)
Bloom J. S., Frail D. A., Kulkarni S. R., 2003, ApJ, 594, 674
Blustin A. J. et al., 2005, GCN 3093
Burrows D. N. et al., 2004, Proc. SPIE, 5165, 201
Burrows D. N. et al., 2005, Space Sci. Rev., in press (astro-ph/0508071)
Bykov A. M., Mészáros P., 1996, ApJ, 461, L37
Campana S. et al., 2005, ApJ, 625, L23
Chevalier R. A., Li Z. Y., 1999, ApJ, 520, L29
Dai Z. G., Cheng K. S., 2001, ApJ, 558, L109
De Luca A., Campana S., 2005, GCN 3109
Dickey J. M., Lockman F. J., 1990, ARA&A, 28, 215
Frail D. A. et al., 2001, ApJ, 562, L55
Gehrels N. et al., 2004, ApJ, 611, 1005
Giommi P. et al., 2005, GCN 3054
Gonzalez-Riestra R. et al., 2005, GCN 3060
Gorosabel J. et al., 2005, GCN 3061
Gronwall C. et al., 2005, GCN 3057
Lamb D. Q., Reichart D. E., 2000, ApJ, 536, 1
Liang E. W., 2004, MNRAS, 348, 153
Mereghetti S., Gotz D., Mowlavi N., Shaw S., Beck M., Borkowski J., 2005, GCN 3059
Mitani T. et al., 2005, GCN 3055
Nysewander M. et al., 2005, GCN 3067
Panaitescu A., Kumar P., 2001, ApJ, 560, L49
Panaitescu A., Mészáros P., 1999, ApJ, 526, 707
Piran T., 1999, Phys. Rep., 314, 575
Piro L., 2004, in ASP Conf. Ser. Vol. 312, 4th workshop on Gamma-Ray Bursts in the Afterglow Era, in press (astro-ph/0402638)
Rodriguez P., 2005, GCN 3065
Roming P. W. A. et al., 2004, Proc. SPIE, 5165, 262
Roming P. W. A. et al., 2005, Space Sci. Rev., in press (astro-ph/0507413)
Rossi E., Lazzati D., Rees M. J., 2002, MNRAS, 332, 945
Sari R., Piran T., Narayan R., 1998, ApJ, 497, L17
Sari R., Piran T., Halpern J. P., 1999, ApJ, 519, L17
Sazonov S. Y., Lutovinov A. A., Sunyaev R. A., 2004, Nat, 430, 646
Smith D., 2005, GCN 3056
Zhang B., Mészáros P., 2002, ApJ, 571, 876
Zhang B., Mészáros P., 2004, Int. J. Mod. Phys, 19, 2385

This paper has been typeset from a TEX/LATEX file prepared by the author.